Structure of charged colloids under a wedge confinement

B. V. R. Tata,[1] Dezsö Boda,[2] D. Henderson,[3] A. Nikolov,[4] and D. T. Wasan[4]
[1]*Materials Science Division, Indira Gandhi Centre for Atomic Research, Kalpakkam 603 102, Tamil Nadu, India*
[2]*Department of Physical Chemistry, University of Veszprem, P.O. Box 158, H-8201 Veszprem, Hungary*
[3] *Department of Chemistry and Biochemistry, Brigham Young University, Provo, Utah 84602-5700*
[4]*Department of Chemical Engineering, Illinois Institute of Technology, Chicago, Illinois 60616*
(Received 16 February 2000)

Monte Carlo simulations have been performed to study the influence of a wedge confinement by hard walls on the ordering of charged colloidal particles interacting through screened Coulomb repulsive potential in an aqueous medium. The density distribution of particles for a fixed wedge angle θ_0 is studied for different suspension parameters, viz., bulk volume fraction ϕ, salt concentration C_s, and charge Ze on the particles. The density distribution $\rho(\theta)$ along the angular direction and that along the radial direction, $\rho(r)$, have been analyzed in different regions of the wedge. Simulations show the formation of layered structure along the angular direction and a large gathering of particles along the wall. The number of layers as well as the density of particles within the layer are found to change as the strength and range of the interaction are varied, whereas the density profiles calculated close to the vertex region showed no significant variation in the density. The radial density profiles $\rho(r)$ corresponding to the vertex region show one-dimensional (1D) ordering of particles parallel to the vertex at a distance that is close to a wedge height, h equal to diameter of the particle. This 1D ordering is found to be destroyed upon the addition of salt or lowering the ϕ. The reported experimental observations on the ''vacuum phase'' are discussed in the light of the present results.

PACS number(s): 82.70.Dd, 64.70.Pf

I. INTRODUCTION

Complex fluids such as colloidal suspensions, micellar solutions, emulsions, etc., in their practical applications involve various environments that correspond to different kinds of confinements [1]. These fluids experience confinement in many ways: (a) fluids inside a porous material or thin cylinderical or spherical cavities, (b) confined by two parallel smooth surfaces, and (c) a wedge formed by two plane surfaces or a spherical and a plane surface. The conditions imposed by confinement have a significant influence on the interactions between particles dispersed in suspensions [2–4], structural ordering [5–10], and phase transitions [11,12]. This influence arises due to the interplay between the intrinsic length scale of the fluid and that of the confinement.

Difficulties in studying the equilibrium properties of confined atomic or molecular fluids generally arise from the small size of the particle as well as the small gap sizes required to observe the structure and measure the properties. However, aqueous suspensions of charged colloidal particles offer several advantages over other complex systems in investigating the effect of confinement on the equilibrium structure and associated properties [5,7,11]. The advantages are (a) due to the particle size being the order of wavelength of visible light, making the particles readily observable using microscopic techniques or by light scattering techniques and (b) due to the easy tunability of interparticle interaction. The latter advantage allows one to study the structural ordering and phase transitions in a bulk suspension of monodisperse charged particles at ambient conditions [13,14]. The interparticle interaction $U(r)$ between the charged colloids is predominantly the screened Coulomb repulsion describable by Derjaguin-Landau-Vervey-Overbeek (DLVO) theory [15]. The potential $U(r)$ can be tuned by varying the suspension parameters, viz., volume fraction ϕ, salt concentration C_s, and effective charge Ze on the particles and realizing crystalline, liquidlike, and even glasslike phases [16] that are analogous to atomic systems. The phase behavior of homogeneous suspensions has been understood based on DLVO potential [13,14,17–19]. Observations on inhomogeneous suspensions, which exhibited gas-liquid [13,20], gas-solid transitions [21], and stable voids coexisting with disordered regions [22,23] could not be understood using DLVO theory. These observations have been understood [21,24,25] based on an effective pair potential having a long-range attractive term given by Sogami-Ise theory. However, its validity is still being debated [13,26]. It has been shown recently that the observations on inhomogeneous suspensions can also be understood based on screened Coulomb repulsive potential between macroions together with additional terms arising due to neutralizing background [27,28].

The DLVO potential has been used to understand the structure formation in a colloidal suspension in the vicinity of a charged wall [8]. These studies show that the displacement of the local structure formation away from the wall is determined by the repulsive wall with a finite charge density and the local structure is determined by the properties of the bulk suspension. Recently, Hug *et al.* [11] have simulated charged colloids confined between two parallel like-charged surfaces and studied the effect of confinement on the freezing volume fraction. Crystallization is found to take place at a lower volume fraction as compared to the bulk freezing volume fraction and a strong dependence of the freezing transition on preferred wall separation corresponding to an integral number of layers. Similarly, when two surfaces (walls) are closely spaced, capillary crystallization or capillary condensation can take place depending on the concen-

tration of the particles experiencing confinement.

Among the various types of confinement, wedge confinement has particular importance as it allows one to study the structural ordering and associated structural transitions in one, two, and three dimensions. In addition to this fundamental interest, the studies on confined colloids under wedge geometry has direct relevance to diverse applications from oil recovery to pollutant removal. Despite its importance, there exist only a few experimental investigations on colloids under wedge confinement [5,6]. In these investigations, the attention has been on formation of thin colloidal crystals and the structures associated with them. Thin colloidal crystals have been produced by confining bulk suspensions within small-angled wedges of two flat glass plates or a flat plate and a glass sphere. In place of a glass sphere, an air bubble has been created by blowing air through the suspension [7]. Such confined suspensions also showed formation of thin colloidal crystals. Observations made as a function of wedge thickness h revealed a sequence of structures that are stacks of n square or triangular ordered layers. The sequence as well as the stacking are found to depend on the wedge thickness and suspension parameters. In the case of highly charged particles, a disordered structure is found for larger values of h and an ordered phase for smaller values of h [7].

These interesting observations on charged colloids have motivated us to study aqueous charged colloids confined under a wedge geometry. Further, there are no simulation studies on charged colloids under a wedge confinement except a recent study by Boda *et al.* on hard spheres [9]. The Monte Carlo (MC) program used here is similar to that employed by Boda *et al.* and is modified to study charged colloids subjected to a wedge confinement. After reaching equilibrium, the density profiles $\rho(\theta)$ as a function of θ and $\rho(r)$ along the radial direction r have been obtained. In this paper, we discuss the behavior of the density profiles calculated around the vertex regions and a region far away from the wedge (toward the end of wedge) for different suspension parameters for a fixed wedge angle. The experimental results are also discussed in light of the present simulation results. The paper is organized as follows.

The details of MC simulation are given in Sec. II. Section III deals with the results of simulations carried out for different suspension parameters and the comparision with the reported experimental observations. A brief summary of the results is given in Sec. IV.

II. DETAILS OF SIMULATION

MC simulations based on Metropolis algorithm for a canonical ensemble (constant N V T, where N, V, and T are, respectively, the number of particles, volume, and the temperature) are carried out with periodic boundary conditions applied along the z direction of the wedge shown in Fig. 1(a). The volume V of the wedge-shaped MC cell is given by $R_0^2\theta_0 Z_0$. Here, R_0, θ_0 and Z_0 define, respectively, the length of the cell in the radial direction, wedge angle θ_0, and length of the wedge along the z direction. Confinement arises due to the hard walls placed at $\theta = \pm\theta_0/2$ and $r = R_0$. The volume V is fixed from the relation $V = N\pi d^3/6\phi$, where ϕ is the required volume fraction $\phi(=\pi d^3 n_p/6)$ of the suspension with particles of diameter d and concentration n_p. In the MC

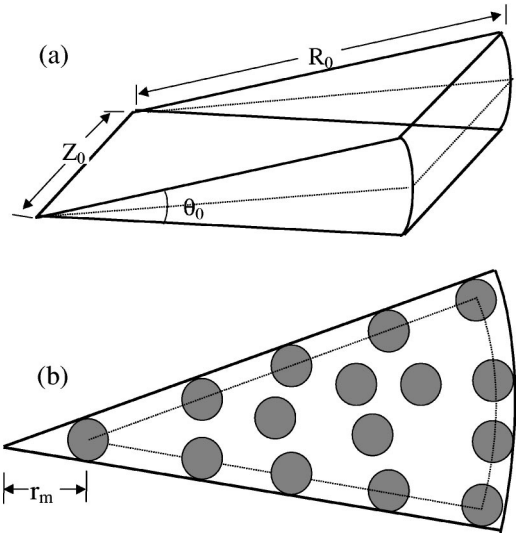

FIG. 1. (a) Schematic of the Monte Carlo cell, where particle centers (r,θ,z) can assume values between $0<r<R_0$, $0<\theta<\theta_0$, and $0<z<Z_0$. The dotted line defines that the wedge is symmetrical about $\theta=0$ and the walls are at $\theta=\pm\theta/2$. (b) The side view of a wedge cell with hard walls confining the particles of diameter d. The dashed line corresponds to the side view of the MC cell.

cell shown in Fig. 1(a), the centers of the particles can be on the vertex of the MC cell. But in an actual (experimental) wedge cell [Fig. 1(b)], the particles of size d cannot approach the vertex except to a minimum radial distance r_m given by the condition $h/d=1$, i.e., $r_m = d/\theta_0$. Hence, for making comparison of simulation results with experiments, r_m has to be added to r to obtain the actual radial distance r_a, i.e., $r_a = r_m + r$. For a wedge angle of 0.5° and $d=1.01$ μm, $r_m/d = 114.6$ and this has been added to r while presenting the $\rho(r)$ curves discussed in Sec. III.

The charged particles in the aqueous suspension confined by the wedge geometry are assumed to interact via the screened Coulomb repulsive pair-potential $U(r)$ [15], which has the form

$$U(r') = \frac{(Ze)^2}{\epsilon}\left(\frac{e^{\kappa a}}{1+\kappa a}\right)^2\left(\frac{e^{-\kappa r'}}{r'}\right) \tag{1}$$

for interparticle distances $r'>d$ and $U(r')=\infty$ for $r'<d$. The inverse Debye screening length κ is given as

$$\kappa^2 = \frac{4\pi e^2}{\epsilon k_B T}(n_p Z + C_s), \tag{2}$$

where Ze is the effective charge on the particle with radius $a=d/2$, C_s is the salt concentration, T the temperature (298 K), ϵ, the dielectric constant of water, and k_B is the Boltzmann constant [29].

Generation of the initial random configuration and MC movement of the particles are done using the linked cell (LC) method [30]. The LC method saves considerable computer time as the overlap checking is straightforward [30] and hence, simulations can be performed with large N. In the present simulations, we have used N ranging from 820 to 4377 to vary the ϕ about an order of magnitude starting from 0.03. Particle diameter d is taken to be 1.01 μm. Simulations

TABLE I. Suspension parameters: Volume fraction ϕ, charge number Z, salt concentration C_s, the inverse Debye screening length (κ), and the number of particles N used in the MC cell.

ϕ	Z	$C_s(\mu\,\mathrm{M})$	κd	N
0.07	33 000	1	7.111	1225
0.12	33 000	1	8.874	2100
0.20	33 000	1	11.13	3501
0.25	33 000	1	12.33	4377
0.07	7 000	1	4.412	1225
0.07	14 000	1	5.276	1225
0.07	20 000	1	5.917	1225
0.07	40 000	1	7.676	1225
0.07	33 000	3	8.529	1225
0.07	33 000	5	9.745	1225
0.07	33 000	10	12.27	1225
0.07	33 000	15	14.35	1225

have been carried out for different values of Ze and C_s and the density profiles $\rho(r)$ and $\rho(\theta)$ have been calculated after reaching the equilibrium. Constancy of the total interaction energy is taken to be the criterion for reaching equilibrium. Typically, 10 000 MC steps (MCS) have been left out for reaching the equilibrium and 15 000 steps have been used for averaging $\rho(r)$ and $\rho(\theta)$, where an MC step is defined as the set of N configurations during which on an average each particle gets a chance to move. The density profile $\rho(\theta)$ along the angular direction is calculated for particles whose r coordinates lie between r_1 and r_2 (where r_1, r_2 take values $0<r_1, r_2<R_0$) and in the angular region $\Delta\theta$ is given by

$$\rho(\theta)=\frac{\langle N(r,z)\rangle}{V_\theta}, \tag{3}$$

where $\langle N(r,z)\rangle$ is the average number of particles that lie within a wedge slice of volume $V_\theta=(r_2^2-r_1^2)\Delta\theta Z_0$.

The density profile $\rho(r)$ along the radial direction is obtained by

$$\rho(r)=\frac{\langle N(\theta,z)\rangle}{V_r}, \tag{4}$$

where $\langle N(\theta,z)\rangle$ is the average number of particles that lie within a wedge slice of volume $V_r=(\Delta r)^2\theta_0 Z_0$. Simulations results reported in this paper correspond to a wedge angle $\theta_0=0.5°$, $R_0=458.37d$, $Z_0=10d$, and the wedge height $h=r\theta_0$ and its value at the end of wedge is $4d$. The wedge angle chosen in the simulations is close to that used in the experiments [5,7].

III. RESULTS AND DISCUSSION

In experiments with wedge geometry [5–7], suspension parameters are chosen such that bulk suspensions undergo crystallization. The suspension parameters chosen in our simulations are given in Table I. For these parameters, we performed MC simulations on bulk suspensions and confirmed that the suspensions exhibit crystallization for salt concentrations less than 3 μM. Since the wedge angle used is very small, the widening of the wedge is too gradual.

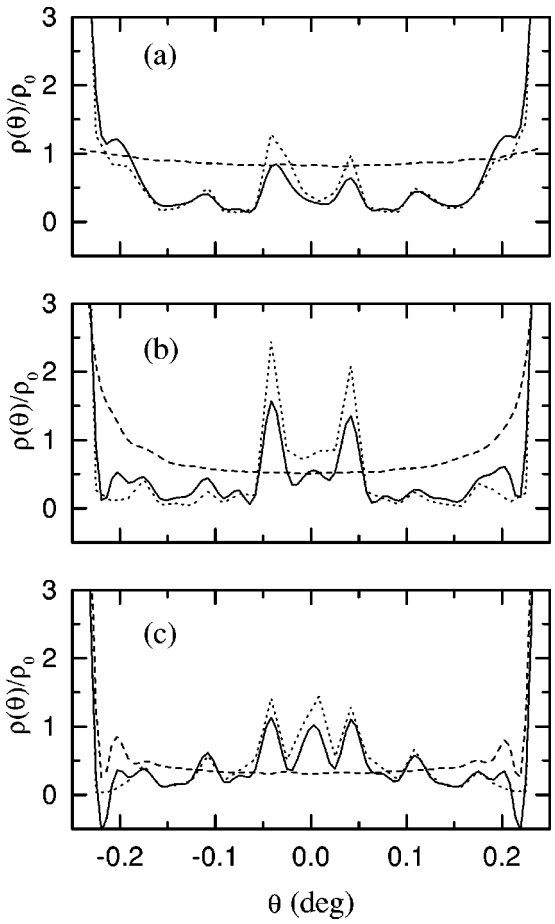

FIG. 2. $\rho(\theta)/\rho_0$ vs θ for volume fractions (a) $\phi=0.07$, (b) $\phi=0.12$, and (c) $\phi=0.20$. The other suspension parameters used in the simulation are $Z=33\,000$, $C_s=1\ \mu M$. The dashed curve corresponds to the vertex region defined by $0<r<R_0/3$; the dotted curve is for the region toward the end of wedge defined by $2R_0/3<r<R_0$; the full curve corresponds to the entire wedge defined by $0<r<R_0$. The maximum values of $\rho(\theta)/\rho_0$ at $\theta=\pm0.242°$ for continuous and dotted curves are in (a) 6.92 and 7.46, (b) 8.86 and 8.84, and (c) 9.63 and 8.1, respectively. The y axis is truncated at 3 for the sake of clarity.

Hence, for making noticeable changes in the density profiles, we divide the entire wedge into three regions, viz., (1) close to the vertex, where r coordinate of the particles lies between 0 to $R_0/3$; (2) the middle region of the wedge, where r coordinates of the particles lie in between $R_0/3$ to $2R_0/3$; and (3) an end region of wedge, where r coordinates of the particles lie in between $2R_0/3$ to R_0. The density distribution functions $\rho(\theta)$ and $\rho(r)$ have been calculated using Eqs. (3) and (4), respectively. The averaging is performed over particle configurations corresponding to 15 000 MCS and the normalization is done with respect to the average density $\rho_0(=N/V)$.

In this paper, we restrict the discussion on the effect of wedge confinement at regions close to the vertex and toward the end of the wedge. Figure 2 shows the density profiles for different values of ϕ. The density profiles are nearly symmetric with respect to the wedge angle zero and are due to the symmetry of the wedge cell [see Fig. 1(a)]. The concave shape of the density profiles of the vertex region suggests that the density of particles closer to the walls is higher than

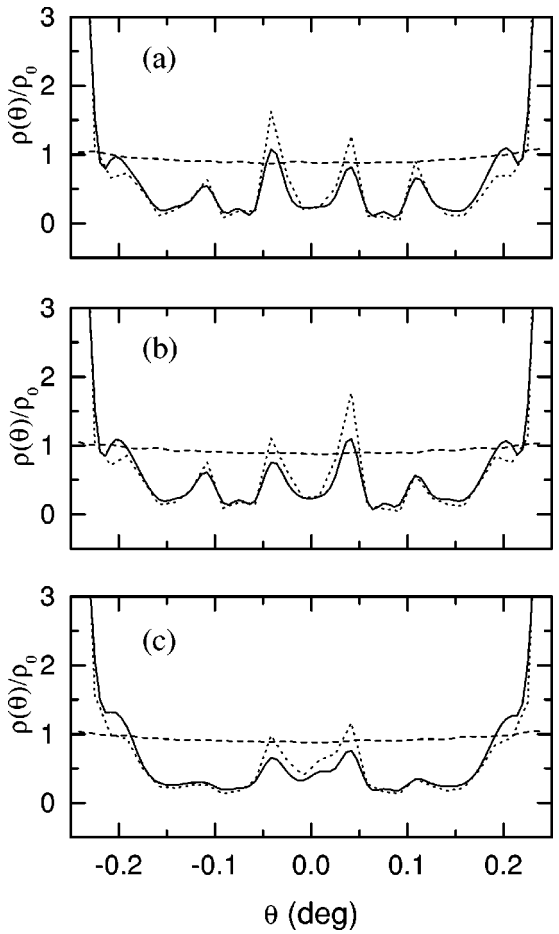

FIG. 3. $\rho(\theta)/\rho_0$ vs r for different charge numbers (a) $Z=14\,000$, (b) $Z=20\,000$, and (c) $Z=40\,000$. The other suspension parameters used in the simulation are $\phi=0.07$, $C_s=1\ \mu M$. The dashed curve, dotted curve, and full curve represent regions of the wedge defined as in Fig. 2. The maximum values of $\rho(\theta)/\rho_0$ at $\theta=\pm 0.242°$ for continuous and dotted curves in (a) 7.54 and 8.05, (b) 7.41 and 7.76, and (c) 6.65 and 7.58, respectively. The y axis is truncated at 3 for the sake of clarity.

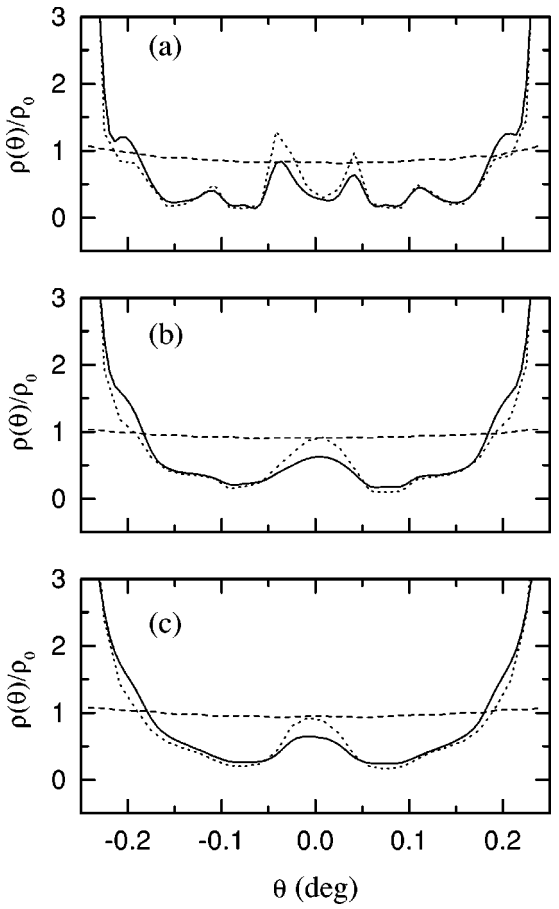

FIG. 4. $\rho(\theta)/\rho_0$ vs r for different salt concentrations (a) $C_s=1\ \mu M$, (b) $C_s=3\ \mu M$, and (c) $C_s=5\ \mu M$. The other suspension parameters used in the simulation are $\phi=0.07$, $Z=33\,000$. The dashed curve, dotted curve, and full curve represent regions of the wedge defined as in Fig. 2. The maximum values of $\rho(\theta)/\rho_0$ at $\theta=\pm 0.242°$ for continuous and dotted curves in (a) 6.85 and 7.41, (b) 5.44 and 6.23, and (c) 4.17 and 4.85, respectively. The y axis is truncated at 3 for the sake of clarity.

at the central region of the wedge. The steepness of the concave shape that indicates the gradient in the density of the particles from the wall to the center of the wedge depends strongly on ϕ. Density profiles corresponding to the end of the wedge show significant structure indicating formation of well-defined layers of particles. Strong peaks at around $\theta=\pm 0.05°$ indicate formation of dense layers closer to the center of the wedge. Other shallow peaks at intermediate angles represent formation of layers that are relatively low in density. Also notice from Fig. 2 the shift in peak positions to lower angles and appearence of a few new peaks as ϕ is increased from 0.07 to 0.2. The shift in peak positions to lower angles suggests the reduction in the interlayer distance. The appearence of new peaks suggests the formation of new layers that lie in between the existing layers in the wedge. Further, the peak heights also are found to change as ϕ is varied. This is due to the variation in the number of particles in each layer and redistribution of particles from one region to another within the wedge or from one layer to the other. The density profiles corresponding to the entire wedge are almost similar to those corresponding to the end of wedge. Since the number of layers that can form in the middle region of the wedge are not more than two, the layered structure that occurs in the end region of the wedge is similar to that of the entire wedge.

In charge stabilized suspensions, the charge on the particle and the corresponding counterions strongly influence the structure formation in bulk suspensions. The effect of wedge confinement on suspensions with particles of increased charge is shown in Fig. 3. It may be mentioned here that the charge on the particles can be tailored experimentally without changing the size of the particles [31]. Also notice from Eqs. (1) and (2) that the strength as well as the range of interaction between the particles become enhanced as the charge on the particles is increased. It can be seen from Fig. 3 that the density profiles corresponding to the vertex region for all vales of Z is the same. Upon increasing Z from 14 000 to 40 000, a shallow peak appears at around $\theta=0°$ in the density profile corresponding to the entire wedge and the end region of the wedge [Fig. 3(c)]. Also notice the reduction in the height of other peaks. These observations suggest that upon increasing charge on the particles, new layers can form at the expense of other layers, as there is no change in the number of particles while Z is increased in simulations.

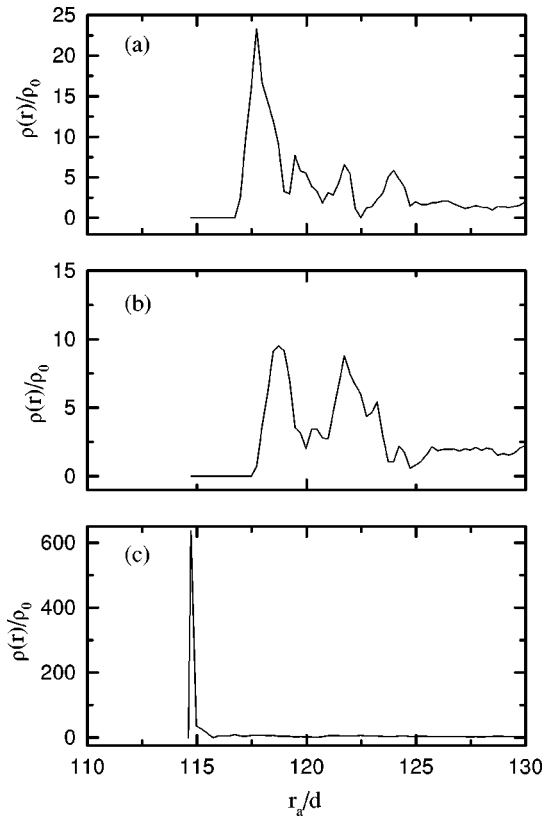

FIG. 5. $\rho(r)/\rho_0$ vs r_a close to the vertex region for volume fractions (a) $\phi=0.07$, (b) $\phi=0.12$, and (c) $\phi=0.20$. The other suspension parameters used in the simulation are $Z=33\,000$, $C_s=1\ \mu M$.

Figure 4 shows the density profiles for different salt concentrations keeping other parameters of the suspension fixed. The density profiles corresponding to the vertex region do not show any change with increase in C_s, whereas those corresponding to other regions of the wedge show deterioration in the layered structure (i.e., reduction in the number of peaks). Apart from the density being high close to the wall there are no other layers except at $\theta=0$ for $C_s>3\ \mu M$. This central peak is found to be very small at a salt concentration of 10 μM (not shown in the figure). Further it can be seen that the density profiles corresponding to the entire wedge exhibit very little structure at $C_s=5\ \mu M$ as compared to that at $1\ \mu M$. These observations suggest that the confinement has lesser influence on weakly interacting colloids as compared to strongly interacting suspensions. We have also carried out simulations on bulk suspensions for the same salt concentrations and found that the suspensions that were crystalline at $C_s<3\ \mu M$ melt into a liquidlike order for $C_s>3\ \mu M$. So the density profiles (Fig. 4) corresponding to $C_s=3\ \mu M$ and $5\ \mu M$ represent formation of a layered fluid in the wedge.

Apart from $\rho(\theta)$, the other density profile that is of interest is the radial density profile $\rho(r)$ as a function of r. The $\rho(r)$ curves corresponding to the entire wedge are found to be highly noisy and hence not presented here. The curves are noisy because in a wedge geometry, as one moves from the vertex to the wedge end, the amount of uncertainty in calculating $\rho(r)$ at large r increases due to the increase in wedge thickness, in other words the decrease in the number of particles per unit volume. Hence we confine our discussion to the $\rho(r)$ corresponding to the vertex region. Further, this region of $\rho(r)$ is of interest because it is possible to make comparison with the occurrence of ''vacuum phase'' that has been observed in experiments [5]. Shown in Fig. 5 is the behavior of $\rho(r)$ versus r_a for suspensions with increasing ϕ. We have shown $\rho(r)$ as function of r_a instead of r due to the difference in the radial distance between the actual wedge and the MC cell (see Fig. 1). It can be noticed from Fig. 5 that the particles have not approached a distance $r_a/d=114.6$ except for $\phi=0.2$. The peaks are also shallow and peak heights are much smaller than those corresponding to $\phi=0.2$. The sharp peak corresponding to $\phi=0.2$ occurring at $r_a/d=114.6$ (i.e., $h/d=1$) suggests that the particles have approached the minimum possible radial distance (touching both walls of the actual wedge) and they are well aligned (1D chain) along the z direction. This is shown schematically in Fig. 6(a). In contrast, particles corresponding to the lower ϕ values are not well ordered (do not form a 1D chain) along the z direction and also occur at a distance larger than $114.6d$ [see Fig. 6(b)]. It is worth mentioning here the experimental observations of Pieranski *et al.* of ''vacuum'' phase (the region bounded by vertex and the first monolayer close to the vertex) and its boundary dependence on the concentration of the samples [5]. They reported formation of a monolayer (first transition from 0 to 1D) in an aqueous suspension of 1.1-μm sized particles confined at a wedge angle of 10^{-2} rad($=0.57°$) at a distance of $h=2.2\ \mu$m (i.e., $h/d=2$) in the concentrated samples and $h=1.6\ \mu$m (i.e., $h/d=1.45$) in the less concentrated sample. Thus our simulations confirm the existence of vacuum phase in dilute charge-stabilized suspensions and its boundary dependence is in agreement with experimental observations.

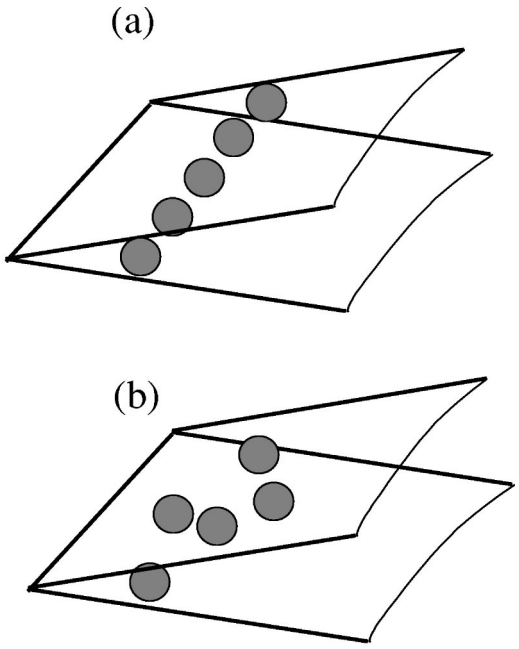

FIG. 6. Schematic of (a) 1D ordering of particles and (b) the disorder in 1D chain of particles close to the vertex region in the MC cell.

In order to know the effect of other suspension parameters, viz., charge on the particle and the salt concentration

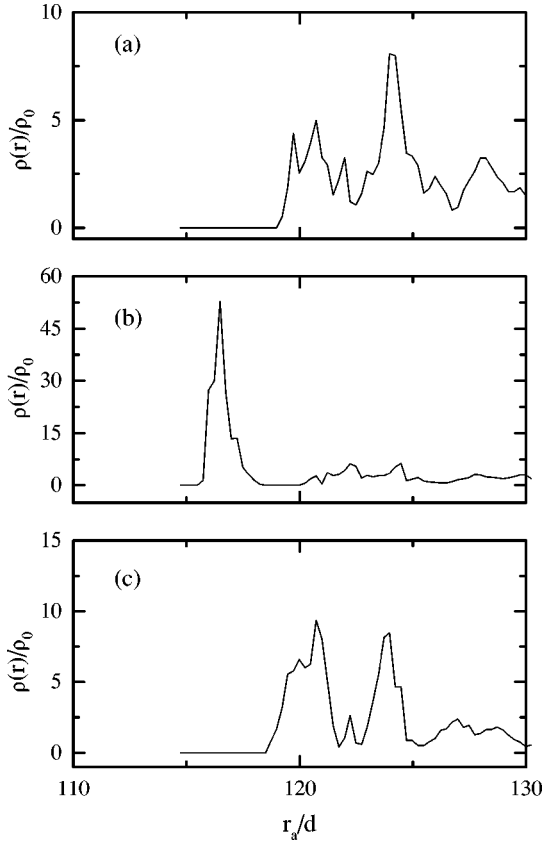

FIG. 7. $\rho(r)/\rho_0$ vs r_a close to the vertex region for different charge numbers (a) $Z=14\,000$, (b) $Z=20\,000$, and (c) $Z=40\,000$. The other suspension parameters used in the simulation are $\phi=0.07$, $C_s=1\ \mu M$.

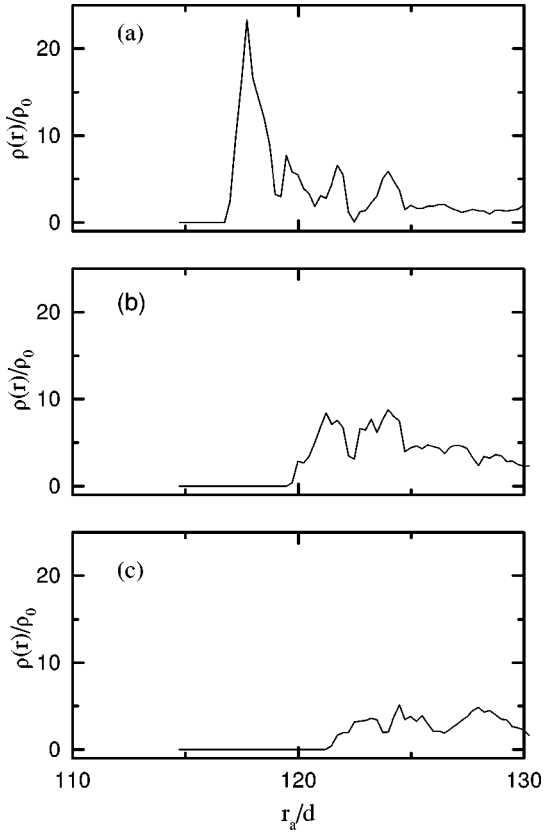

FIG. 8. $\rho(r)/\rho_0$ vs r close to the vertex region for different salt concentrations (a) $C_s=1\ \mu M$, (b) $C_s=3\ \mu M$, and (c) $C_s=5\ \mu M$.

on the vacuum phase, we calculated the density profiles close to the vertex region and these are shown in Figs. 7 and 8. Notice that the peaks for $Z=14\,000$ and $40\,000$ are much smaller compared to that for $Z=20\,000$ and the position at which $\rho(r)$ becomes nonzero for the first time (formation of monolayer) is $\sim 120d$ for $Z=14\,000$ and $40\,000$, which is higher compared to $\sim 115d$ for $Z=20\,000$. The higher peak height for $Z=20\,000$ suggests significant 1D ordering of particles in the monolayer as compared to the ordering (shallow peaks) of particles corresponding to $Z=14\,000$ and $40\,000$. In other words, ordering as well as the boundary of the vacuum phase have a nonmonotonic dependence on the charge on the particles, whereas it can be seen from Fig. 8 that the boundary of the vacuum phase shifts to higher values of r_a as the salt concentration is increased in the suspension. Further, the absence of any peak for $C_s>3\ \mu M$ suggests that no ordering of particles occur at the boundary of the vacuum phase.

The occurrence of 1D ordering and the shift in boundary of the vacuum phase can be understood from the following qualitative arguments. The addition of salt decreases the strength of interaction and hence the bulk suspensions at high salt concentration exhibit only short-range (liquidlike) order. In fact, our simulations on bulk suspensions for the same suspension parameters showed crystalline order for $C_s=1\ \mu M$ and liquidlike order for $C_s>3\ \mu M$. The liquidlike ordered suspensions, when confined in a wedge, exhibited layering (see Fig. 5). The layering arises due to the competition between the confinement force arising due to the walls and the normal component of the virial force arising due to the screened Coulomb interaction between the particles. The radial component of the force is expected to be responsible for the ordering of particles close to the vertex. The strength of this component of the force is dictated by the strength of the interparticle interaction. As the salt concentration is increased, the strength of interaction between particles comes down due to the increase in κ. As a result, the particles cannot experience sufficient force to reach the minimum radial distance r_m and also cannot undergo 1D ordering parallel to the vertex. The simulation results with variation in C_s (see Fig. 8) provide evidence for this.

In contrast, in suspensions with low salt concentration, particles interact strongly, hence can compete with the confinement force. The strength of interparticle interaction can also be increased monotonically either by increasing ϕ or the charge on the particles. Such strongly interacting suspensions exhibit significant structure (see Figs. 2 and 3) under wedge confinement. The subtle interplay between the wedge angle and the structure induced in the system by the walls of the wedge seems to be responsible for the nonmonotonic shift in the boundary of the vacuum phase and the occurrence of 1D ordering near the vertex (see Figs. 5 and 7). Though the closest radial distance to which that particle of diameter d can approach is set by the condition $h/d=1$, the actual radial distance to which the charged colloidal particles in a suspension can approach toward the vertex and the ordering exhibited at that distance is dictated by the wedge angle and the confinement- induced structure in the rest of

the wedge. Further simulations on systems of larger sizes with different wedge angles and with different wall particle interactions are expected to throw more light (a) in understanding the boundary behavior of the vacuum phase, (b) on the circumstances that bring 1D ordering, and (c) for making quantitative comparison with experimental observations.

IV. SUMMARY

To summarize, we have simulated charged colloids interacting through screened Coulomb repulsion confined by hard walls forming a wedge geometry. The layering formation for different suspension parameters has been characterized by analyzing the density profiles $\rho(\theta)$ calculated along the wedge angle for different regions of the wedge. The formation of a layered structure is established from the occurrence of peaks in $\rho(\theta)$ versus θ corresponding to the end of the wedge region. The analysis of the density profiles, $\rho(r)$ versus r, corresponding to the vertex region revealed (a) formation of an ordered 1D chain (particles aligned along the z direction of the wedge) and a disordered 1D chain leading to the formation of monolayer of particles at higher r. The behavior of these density profiles for different suspension parameters and from the results obtained by performing simulations on bulk suspensions has allowed us to locate the position of the boundary of the vacuum phase and compare with experimental observations. The results are understood based on our own simulation results on the bulk suspensions and analyzing the dependence of the shift of the vacuum-phase boundary and the occurrence of 1D ordering of particles close to the vertex. Calculations of inlayer structure at different values of h along the wedge are expected to provide further insight into the sequence of structures and their stacking observed in experiments with a wedge confinement.

ACKNOWLEDGMENTS

This work was supported in part by the U.S. Department of Energy (Grant No. DE-FG07-97ER14828), the National Science Foundation (Grants Nos. 96-01971, 98-13729, and CTS-9423584), and by the donors of the Petroleum Research Fund, administered by the American Chemical Society (Grant No. ACS-PRF 31573-AC9). We thank Dr. A. K. Arora for helpful discussions.

[1] S.Hj. Idziak and Y. Li Curr. Opin. Colloid Interface Sci. **3**, 293 (1998).
[2] J.C. Crocker and D.G. Grier, Phys. Rev. Lett. **77**, 1897 (1996); G.M. Kepler and S. Fraden, *ibid.* **73**, 356 (1994).
[3] W.R. Bowen and A.O. Sharif, Nature (London) **393**, 663 (1998); J.C. Neu, Phys. Rev. Lett. **82**, 1072 (1999).
[4] K. Srinivasa Rao and R. Rajagopalan Phys. Rev. E **57**, 3227 (1998).
[5] P. Pieranski, L. Strzeleci, and B. Pansu Phys. Rev. Lett. **50**, 900 (1983); B. Pansu *et al.*, J. Phys. (France) **44**, 531 (1983).
[6] C.A. Murray and D.H. Van Winkle, Phys. Rev. Lett. **58**, 1200 (1986); C.A. Murry *et al.*, Phase Transit. **21**, 93 (1990).
[7] A.D. Nikolov and D.T. Wasan (private communication).
[8] P. Gonzalez-Mozuelos and M. Medina-Noyola, J. Chem. Phys. **93**, 2109 (1990); **94**, 1480 (1990).
[9] D. Bodal, K.Y. Chan, D. Henderson, D.T. Wasan, and A.D. Nikolov, Langmuir **15**, 4311 (1999).
[10] X.L. Chu, A.D. Nikolov, and D.T. Wasan, Langmuir **10**, 4403 (1994).
[11] J.E. Hug, F. van Swol, and C.F. Zukoski, Langmuir **11**, 111 (1995).
[12] A.H. Marcus and S.A. Rice, Phys. Rev. E **55**, 637 (1997).
[13] A.K. Arora and B.V.R. Tata, Adv. Colloid. Interface Sci. **78**, 49 (1998).
[14] *Ordering and Phase Transitions in Charged Colloids*, edited by A.K. Arora and B.V.R. Tata (VCH, New York, 1996).
[15] E.J.W. Verwey and J.Th.G. Overbeek, *Theory of the Stability of Lyophobic Colloids* (Elsevier; Amsterdam, 1948).
[16] E.B. Sirota, H.D. Ou-Yung, S.K. Sinha, P.M. Chaikin, J.D. Axe, and Y. Fujji, Phys. Rev. Lett. **62**, 1524 (1989); R. Kesavamoorthy, A.K. Sood, B.V.R. Tata, and A.K. Arora, J. Phys. C **21**, 4737 (1988).
[17] R.O. Rosenberg and D. Thirumalai, Phys. Rev. A **36**, 5690 (1987); D. Thirumalai, J. Phys. Chem. **93**, 5637 (1989).
[18] M.O. Robbins, K. Kremer, and G.S. Grest, J. Chem. Phys. **88**, 3286 (1988).
[19] J. Chakrabarti, H. R. Krishanmoorthy, S. Sengupta, and A. K. Sood, in *Ordering and Phase Transitions in Charged Colloids* (Ref. [14]).
[20] B.V.R. Tata and A.K. Arora, in *Ordering and Phase Transitions in Charged Colloids* (Ref. [14]), p. 149.; B.V.R. Tata, M. Rajalakshmi, and A.K. Arora, Phys. Rev. Lett. **69**, 3778 (1992).
[21] B.V.R. Tata and Baldev Raj, Bull. Mater. Sci. **21**, 263 (1998).
[22] K. Ito, H. Yoshida, and N. Ise, Science **263**, 66 (1994).
[23] B.V.R. Tata, E. Yamahara, P.V. Rajamani, and N. Ise, Phys. Rev. Lett. **78**, 2660 (1997).
[24] B.V.R. Tata and N. Ise, Phys. Rev. E **58**, 2237 (1998).
[25] N. Ise, T. Konishi, and B.V.R. Tata, Langmuir **15**, 4176 (1999).
[26] K.S. Schmitz, *Macroions in Solution and Colloidal Suspensions* (VCH, New York, 1993).
[27] R. van Roij, M. Dijkstra, and J.-P. Hansen, Phys. Rev. E **59**, 2010 (1999).
[28] P.B. Warren, J. Chem. Phys. **112**, 4683 (2000).
[29] Y. Monovoukas and A.P. Gast, Langmuir **7**, 460 (1991); Phase Transit. **21**, 183 (1990).
[30] D. Boda, K.Y. Chan, and I. Szalai, Mol. Phys. **92**, 1067 (1997).
[31] J. Yamanaka, T. Koga, N. Ise, and T. Hashimoto, Phys. Rev. E **53**, R4314 (1996); J. Yamanaka, H. Hayashi, N. Ise, and T. Yamguchi, *ibid.* **55**, 3028 (1997).